Endocrine, *vol. 18, no. 3, 221–229, August 2002* 0969–711X/02/18:221–229/$20.00

Intracellular Calcium Ion Response to Glucose in β-Cells of Calbindin-D_{28k} Nullmutant Mice and in βHC13 Cells Overexpressing Calbindin-D_{28k}

Jai Parkash,[1] Muhammad A. Chaudhry,[1] Ayman S. Amer,[1] Sylvia Christakos,[2] and William B. Rhoten[1]

[1]Department of Anatomy, Cell and Neurobiology, Joan C. Edwards School of Medicine, Marshall University, Huntington, WV; and [2]Department of Biochemistry and Molecular Biology, New Jersey Medical School, University of Medicine and Dentistry of New Jersey, Newark, NJ

This article describes studies on the glucose-induced responses of intracellular Ca^{2+} concentration ($[Ca^{2+}]_i$), insulin release, and redistribution of calbindin-D_{28k}, a calcium-binding regulatory protein, in β-cells of pancreatic islets of calbindin-D_{28k} knockout (KO) and wild-type mice (C57BL6) as well as in βHC-13 control cells and βHC-13 CaBP40 cells (β-cell line overexpressing calbindin-D_{28k}). Upon increasing the glucose concentration from 2.8 to 30 m*M*, islets of KO mice showed a significantly greater increase in $[Ca^{2+}]_i$ (mean increase in $[Ca^{2+}]_i$, i.e., $\Delta[Ca^{2+}]_i$, was 296 n*M*) compared with wild-type mice ($\Delta[Ca^{2+}]_i$ = 97 n*M*). βHC-13 CaBP40 cells showed little change in $[Ca^{2+}]_i$ upon elevation of glucose from 5.5 to 32.7 m*M*, whereas βHC-13 control cells exhibited significant increases in $[Ca^{2+}]_i$ ($\Delta[Ca^{2+}]_i$ = 510 n*M*). Similarly, upon addition of 30 m*M* glucose, the rate of insulin release increased from 25.2 (basal rate) to 145.2 pg/mL/min in βHC-13 control cells, whereas in βHC-13 CaBP40 cells the rate of insulin release was only 27.5 pg/mL/min in high glucose. Thus, levels of calbindin-D_{28k} in β-cells affect both $[Ca^{2+}]_i$ and insulin secretion in response to glucose. The three-dimensional reconstruct of confocal immunofluorescent images showed that glucose caused redistribution of calbindin-D_{28k} resulting in co-localization in the region of L-type voltage-dependent calcium channels (VDCC). This co-localization may be an important regulatory function concerning Ca^{2+} influx via L-type VDCC and exocytosis of insulin granules.

Key Words: β-cells; calbindin-D_{28k}; insulin; intracellular Ca^{2+}; islets; knockout mouse.

Introduction

It is now becoming evident from several lines of research that the temporal and spatial regulation of intracellular calcium concentration ($[Ca^{2+}]_i$) is very crucial for maintaining calcium ion homeostasis within cells, and, consequently, in the regulation of various cellular functions such as cell proliferation, differentiation, cytotoxicity, glucose metabolism, and apoptosis *(1–7)*. Calbindins are high-affinity calcium-binding regulatory proteins that have been shown to play important roles in modulating the $[Ca^{2+}]_i$ in various cell types and thus affect several biochemical events within the cell including depolarization-induced insulin secretion by β-cells *(5)*. Calbindin-D_{28k} is comprised of 260 amino acid residues with a molecular weight of 28 kDa and mainly appears to be a cytoplasmic protein belonging to a family of high-affinity calcium-binding proteins such as calmodulin, troponin C, calbindin-D_{9k}, parvalbumin, S100 protein, and secretagogin *(8–12)*. The genomic structure of calbindin-D_{28k}, which is well conserved phylogenetically, consists of 11 exons and 10 introns and in humans the calbindin-D_{28k} gene is located on chromosome 8 (see refs. *13–15*). Calbindin-D_{28k} has at least five high-affinity calcium ion binding sites that originate from six EF hands packed into one glo-bular domain *(16)*. RIN (rat insulinoma 1046-38) cells with elevated levels of calbindin-D_{28k} have increased cytoplasmic Ca^{2+} buffering capacity *(17,18)*. In HEK 293 cells stably transfected with human recombinant calbindin-D_{28k}, Rintoul et al. *(19)* showed that the presence of calbindin-D_{28k} significantly reduced the ionophore 4-Br-A23187 induced rise in $[Ca^{2+}]_i$. Bellido et al. *(20)* have shown that the transient expression of rat calbindin-D_{28k} cDNA in MC3T3-E1 osteoblastic cells inhibited the tumor necrosis factor alpha (TNFα)-induced apoptosis and caspase-3 activity in addition to causing increased calcium buffering, thus showing the anti-apoptotic properties of calbindin-D_{28k}. Therefore, in summary, calbindin-D_{28k} appears to both modulate calcium transients and to protect against cellular degradation *(21,22)*.

In an earlier study *(5)*, we found that following K^+-depolarization (45 m*M* KCl) $[Ca^{2+}]_i$ was significantly greater in isolated pancreatic islets of calbindin-D_{28k} null-mutant

Received April 19, 2002; Revised July 1, 2002; Accepted July 3, 2002.

Author to whom all correspondence and reprint requests should be addressed: Jai Parkash, Ph.D., Department of Anatomy, Cell and Neurobiology, Joan C. Edwards School of Medicine, Marshall University, 1542 Spring Valley Drive, Huntington, WV 25704-9388. E-mail: parkash@marshall.edu

mice compared with wild-type islets. Conversely, βTC-3 and βHC-13 cells overexpressing rat calbindin-D_{28k} showed markedly reduced $[Ca^{2+}]_i$ response to K^+. It was also shown that calbindin-D_{28k} played a regulatory role in depolarization-induced insulin secretion via control of $[Ca^{2+}]_i$. In the present study we explored the effect of glucose, the major nutrient regulator of insulin secretion, on intracellular Ca^{2+} dynamics in calbindin-D_{28k} null-mutant and wild-type pancreatic islets and in βHC-13 cells stably transfected with calbindin-D_{28k}. The results are discussed in the light of calbindin-D_{28k} regulation of intracellular Ca^{2+} and spatial redistribution of this calcium-binding protein vis-à-vis L-type voltage-dependent calcium channels (VDCC).

Results

Glucose-Induced Increase in $[Ca^{2+}]_i$ in WT and KO Islets

Upon addition of 30 m*M* glucose to islets prepared from WT mice, the $[Ca^{2+}]_i$ increased immediately and a peak in $[Ca^{2+}]_i$ was observed about 1–2 min after addition of glucose (Fig. 1A). This peak in $[Ca^{2+}]_i$ was followed by a decline and then a slow rise in $[Ca^{2+}]_i$ to a plateau seen after about 20 min. The maximum increase in $[Ca^{2+}]_i$ in WT islets in response to high glucose ranged between 68 and 120 n*M* (mean increase in $[Ca^{2+}]_i$, $\Delta[Ca^{2+}]_i$, was = 96.7 n*M* with a SEM = ± 8.4 n*M*, n = 7). The initial rate of increase in $[Ca^{2+}]_i$, rate of decline in $[Ca^{2+}]_i$ after attaining the peak, and the rate of slow rise to a plateau value, as well as the magnitude of changes in $[Ca^{2+}]_i$ varied from islet to islet (see Fig. 1A). The basal values of $[Ca^{2+}]_i$ in islets obtained in the presence of 2.8 m*M* glucose remained constant (0–5 min, Fig. 1A), thus showing that the observed increase in $[Ca^{2+}]_i$ upon addition of 30 m*M* glucose is the responsiveness of β-cells of islets to their physiological substrate. As shown in Fig. 1B, exposure of KO islets to high glucose resulted in a rapid and marked transient increase in $[Ca^{2+}]_i$. The time course of this peak was similar to that in WT islets (compare Figs. 1, A and B, note differences in scales). However, the magnitude of the increase in $[Ca^{2+}]_i$ upon addition of high glucose to the KO islets that ranged between 200 and 366 n*M* during 20–25 min ($\Delta[Ca^{2+}]_i = 296.3 \pm 21.2$ n*M*, n = 7) was much greater ($p < 0.001$) than that in WT islets (see Fig. 2).

The absence of calbindin-D_{28k} in KO mice was verified by Western blotting of kidneys (Fig. 3). Kidneys were used for Western blotting because kidneys of WT mice contain much higher levels of calbindin-D_{28k} than do pancreata.

Glucose-Induced Changes in $[Ca^{2+}]_i$ in β-Cell Lines

The basal $[Ca^{2+}]_i$ in control βHC-13 cells ranged between 110 and 154 n*M* (mean basal $[Ca^{2+}]_i = 130 \pm 4$ n*M*, n = 15 cells) and upon addition of 30 m*M* glucose a steady increase in $[Ca^{2+}]_i$ was observed up to about 20 min and then reached a plateau as shown in Fig. 4A. After 21.5 min of addition of high glucose, the $[Ca^{2+}]_i$ ranged between 401 and 681 n*M*, giving an increase in $[Ca^{2+}]_i$ of 290–571 n*M* ($\Delta[Ca^{2+}]_i = 510 \pm 19$ n*M*, n = 15 cells). The rate of increase in $[Ca^{2+}]_i$ upon addition of 30 m*M* glucose to the βHC-13 cells varied among cells from three experiments, but a mean rate of increase in $[Ca^{2+}]_i$, i.e., $d[Ca^{2+}]_i/dt$ was approx 21.5 n*M*/min over the initial 20 min. The pattern of increase in $[Ca^{2+}]_i$ was oscillatory in nature with varying frequencies and amplitudes.

Table 1
Rates of Glucose-Induced Insulin Release from the βHC-13 Control Cells and βHC-13 CaBP40 Cells at 37ºC

Incubations	Rate of Insulin Release (pg/mL/min)[a] βHC-13 control cells	βHC-13 CaBP40 cells
1. 5.5 m*M* Glucose, 2 h	25.2 ± 2.0	5.60 ± 2.0
2. 30 m*M* Glucose, 5 min	145.2 ± 38.1	27.5 ± 1.7
3. 30 m*M* Glucose, 15 min further	62.2 ± 10.0	8.0 ± 1.0

[a] The data expressed as a mean ± SEM are derived from a set of three wells each of βHC-13 control cells and βHC-13 CaBP40 cells.

In βHC-13 CaBP40 cells overexpressing calbindin-D_{28k}, the basal $[Ca^{2+}]_i$ ranged between 51 and 193 n*M* (mean basal $[Ca^{2+}]_i = 125 \pm 14$ n*M*, n = 9). Upon addition of high glucose, no significant change in $[Ca^{2+}]_i$ was observed (mean $[Ca^{2+}]_i = 126 \pm 14$ n*M*, n = 9, the $[Ca^{2+}]_i$ ranged between 41 and 194 n*M*; see Fig. 4B). The basal $[Ca^{2+}]_i$ was similar in βHC-13 CaBP40 cells and control βHC-13 cells.

Glucose-Induced Insulin Release from β-Cell Lines

The basal rates of insulin release determined in the presence of 5.5 m*M* glucose over a period of 2 h at 37ºC were 25.2 and 5.60 pg/mL/min in βHC-13 control cells and βHC-13 CaBP40 cells, respectively (Table 1). During the first 5 min of incubation in 30 m*M* glucose (first or rapid phase of insulin secretion), the rate of insulin release increased significantly to 145.2 pg/mL/min in βHC-13 control cells. In contrast, the rate of insulin release in βHC-13 CaBP40 cells was only 27.5 pg/mL/min over the first 5 min of incubation, which is comparable to basal release in βHC-13 control cells. The incubation of these β-cell lines in high glucose for an additional 15 min resulted in release of insulin at a rate of 62.2 and 7.98 pg/mL/min in βHC-13 control cells and βHC-13 CaBP40 cells, respectively (Table 1).

The Localization, Co-localization, and Interaction among Calbindin-D_{28k}, L-type Ca^{2+} Channels, and Insulin

The dynamics of glucose-induced changes in $[Ca^{2+}]_i$ and its consequences on the interactions between calbindin-D_{28k} and L-type VDCC were analyzed by labeling with fluorescent-tagged secondary antibodies to these proteins in βHC-13 CaBP40 cells treated with 5.5 and 30 m*M* glucose and fixed

in space and time. βHC-13 CaBP40 cells were used to perform this study because this cell line expressed high levels of calbindin-D_{28k} and thus provided significant immunofluorescent signal. Figure 5A is a three-dimensional (3-D) reconstruction of the βHC-13 CaBP40 cells treated with 5.5 m*M* glucose. The L-type channels (shown in green color) were abundant in the plasma membrane as expected and were absent in the cytoplasmic regions (see Fig. 5A). The calbindin-D_{28k} (shown in red color) was primarily localized in the cytoplasm and was mostly homogeneously distributed with scattered focal concentrations (Fig. 5A). When the βHC-13 CaBP40 cells were treated with 30 m*M* glucose, one could observe several areas of yellow coloration in addition to the red and green colors in the 3-D reconstruct of the confocal image (*see* Fig. 5B). The appearance of the yellow color is a direct indication of co-localization of calbindin-D_{28k} and L-type VDCC (red + green = yellow).

In order to show that glucose can induce exocytosis of insulin secretory granules from the KO islets, 3-D reconstructions of confocal images were acquired from KO islets treated with 30 m*M* glucose. Islets exposed to high glucose exhibited decreased cytoplasmic insulin secretory granules compared with those in 2.8 m*M* glucose (compare Fig. 6B with Fig. 6A). In 2.8 m*M* glucose (Fig. 6A), abundant insulin secretory granules (shown in blue color) were present in the cytoplasm with well-defined cell boundries showing L-type VDCC (in green color). After exposure to high glucose for 20 min at 37ºC (Fig. 6B), the 3-D reconstruct showed reduced levels of insulin granules (less blue color) thus indicating the glucose-induced exocytosis of the insulin secretory granules from the KO β-cells.

Discussion

In order to study the role of calbindin-D_{28k} in nutrient-regulated responses of intracellular Ca^{2+} in β-cells, we adopted a two-pronged strategy. First, we used a transgenic null-mutant mouse devoid of calbindin-D_{28k} gene (knock-out, see ref. *6*) Second, we used a β-cell line, βHC-13, stably transfected with an inserted gene that encodes for calbindin-D_{28k}. This cell line known as βHC-13 CaBP40 overexpresses calbindin-D_{28k} *(5,23)*. The results presented in Figs. 1A, B, and 2 show that the $[Ca^{2+}]_i$ response to glucose in KO islets was at least three times greater ($p < 0.001$) as compared to that in WT islets. Our previous studies showed that membrane depolarization induced by addition of 45 m*M* KCl to the islets caused approx 3.5 times more increase in $[Ca^{2+}]_i$ in KO mice islets as compared to that in islets prepared from WT mice *(5)*. Therefore, our present data using glucose as a physiological secretagogue support the previous observation of a several-fold greater increase in $[Ca^{2+}]_i$ in KO islets. The increase in $[Ca^{2+}]_i$ upon addition of glucose (in the present study) or KCl (as in ref. *5*) was transient in nature thereby emphasizing depolarization-induced influx of Ca^{2+} across the cell membrane. The metabolism of glucose via cytosolic glycolysis pathway and the mitochondrial oxidation of the glycolytic products in β-cells of the islets of Langerhans increase the ATP to ADP ratio resulting in the closure of ATP-sensitive K^+ (K^+_{ATP}) channels *(24–31)*. This closure of K^+_{ATP} channels causes membrane depolarization and, consequently, the L-type VDCC are activated leading to influx of Ca^{2+} into the cytoplasm down the electrochemical gradient of Ca^{2+} across the plasma membrane *(32)*. The increase in $[Ca^{2+}]_i$ of β-cells results in exocytosis of insulin secretory granules *(33–35)*. Duchen et al. *(36)* have proposed that an increase in $[Ca^{2+}]_i$ could also lead to an increase in mitochondrial Ca^{2+} concentration, which then enhances the ATP synthesis. As is evident in Figs. 1A, B, the presence of 30 m*M* glucose caused a plateau in $[Ca^{2+}]_i$ in WT mouse islets, and a second peak in $[Ca^{2+}]_i$ in KO mice islets after about 20–25 min. The presence or absence of a plateau in $[Ca^{2+}]_i$ has been reported in several studies involving islets derived from mouse and rat *(30,37,38)*, and could be correlated in the present study to the maintenance of the membrane depolarization state of β-cells by the action of the glucose. The maintenance of membrane depolarization state in β-cells is also dependent on those mechanisms that are involved in the membrane depolarization/ repolarization phase in addition to K^+_{ATP} channels. Such mechanisms include Na^+/Ca^{2+} exchanger, Ca^{2+} sensitive nonselective cation channels, and stimulation of a small voltage-activated outward K^+ current that develops because of influx of Ca^{2+} *(39–41)*. In studies involving Purkinje neurons from calbindin-D_{28k} KO mice, Airaksinen et al. *(6)* have shown a larger amplitude of synaptically evoked calcium ion transients as compared to that in WT mice. Their result correlates well with the larger magnitude of glucose-induced rise in $[Ca^{2+}]_i$ in KO islets as compared to that in WT islets described above in the present study. These observations based on the removal of calbindin-D_{28k} from such diverse cell types as neurons, on the one hand, and β-cells, on the other hand, from KO mice, support a role for calbindin-D_{28k} in the regulation of cellular calcium and Ca^{2+}-dependent processes *(5,6)*.

The results with βHC-13 CaBP40 cells show that overexpression of calbindin-D_{28k} caused almost a complete absence of the typical glucose-induced rise in $[Ca^{2+}]_i$ in these cells. In control βHC-13 cells the addition of high glucose caused a very substantial increase in $[Ca^{2+}]_i$ by 510 ± 19 n*M* (Fig. 4A). The absence of response by βHC-13 CaBP40 cells (Fig. 4B) further supports a role for calbindin-D_{28k} in modulating Ca^{2+}-dependent processes. One mechanism of action of calbindin-D_{28k} in βHC-13 CaBP40 cells may be intracellular calcium buffering. An earlier study with RIN cells demonstrated a large increase in cytoplasmic Ca^{2+} buffering capacity in RIN cells with levels of calbindin-D_{28k} about three-fold higher than in control cells *(17)*. In cells with elevated calbindin-D_{28k} the $[Ca^{2+}]_i$ response to glucose, K^+-depolarization, a calcium ionophore (ionomycin), and Ca^{2+} channel agonist Bay K 8644 were altered, but basal $[Ca^{2+}]_i$ was unchanged. $[Ca^{2+}]_i$ peak values were reduced and the increase in $[Ca^{2+}]_i$

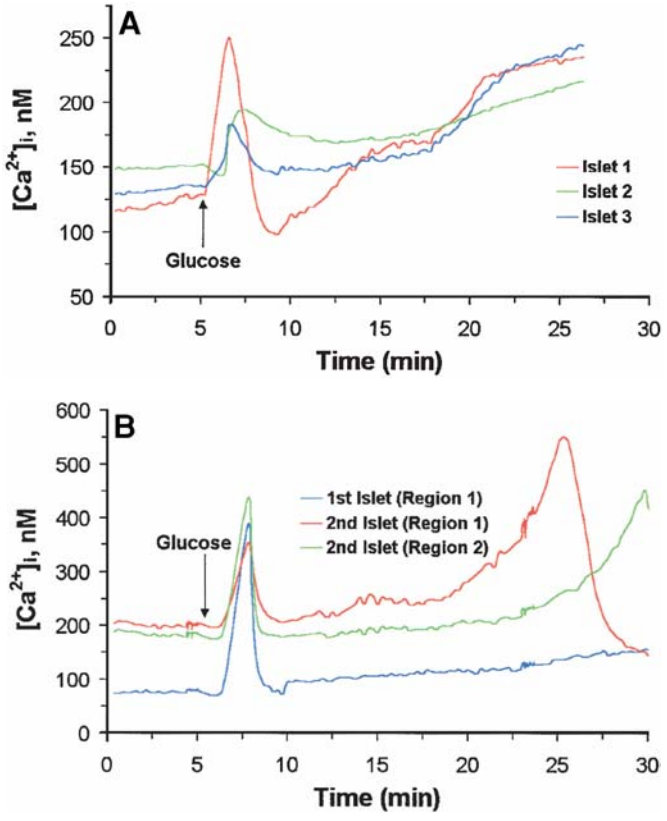

Fig. 1. Kinetics of glucose-induced increase in $[Ca^{2+}]_i$ in WT and KO islets. The (**A**) WT and (**B**) KO islets incubated in a modified Kreb's ringer medium containing 2.8 m*M* glucose were exposed to 30 m*M* glucose (at times shown by arrows) and the time course of changes in $[Ca^{2+}]_i$ was measured using Fura-2 ratio fluorescent microscopy. The increase in $[Ca^{2+}]_i$ upon incubation in high glucose was much greater in KO islets than in WT islets. Note difference in scale of ordinate in **B**.

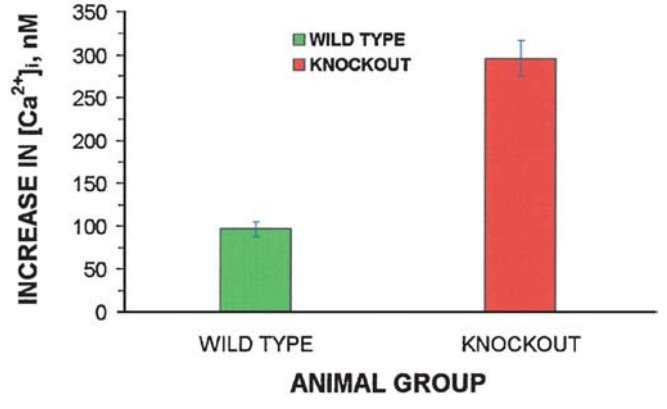

Fig. 2. Maximum increase in $[Ca^{2+}]_i$ in WT and KO islets upon addition of high glucose. A histogram showing the relative glucose responsiveness in WT and KO mice islets as measured by the increase in $[Ca^{2+}]_i$ during the 20th–25th min of incubation (*see* Fig. 1). The maximum increase in $[Ca^{2+}]_i$ in KO islets was about three times more than that in WT islets.

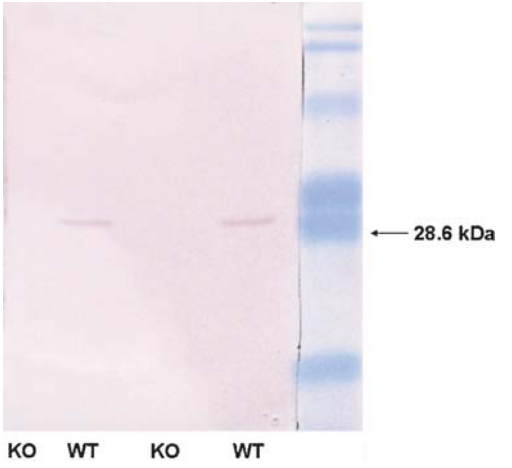

Fig. 3. Absence of calbindin-D_{28k} in KO mice. The Western blot of kidney homogenates from WT (lanes 2 and 4) and KO mice (lanes 1 and 3) carried out using mouse anti-calbindin-D_{28k} antibody shows the absence of calbindin-D_{28k} in KO mice. The standard molecular weight markers are shown in the rightmost lane with M_r (from top to bottom) of 139, 86.8, 47.8, 33.3, 28.6, and 20.7.

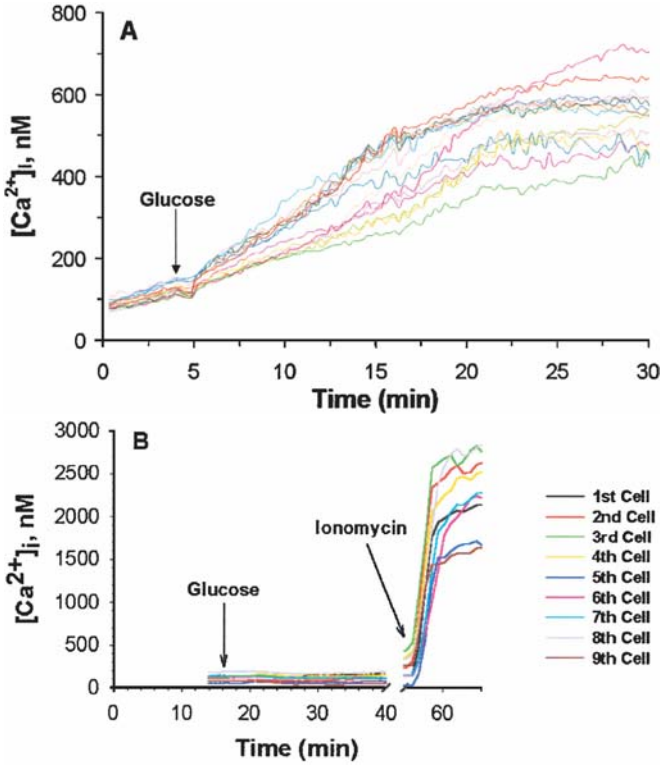

Fig. 4. Glucose-induced changes in $[Ca^{2+}]_i$ in βHC-13 control cells and in βHC-13 CaBP40 cells. **(A)** βHC-13 control cells loaded with Fura-2 ratio fluorescent probe and incubated in HBSS were exposed to 30 m*M* glucose (at time shown by arrow) and the time course of increase in $[Ca^{2+}]_i$ was followed. The $[Ca^{2+}]_i$ data shown are for 15 individual βHC-13 cells. (**B**) βHC-13 CaBP40 cells overexpressing calbindin-D_{28k} incubated in HBSS were exposed to high glucose (at time shown by arrow) and the time course of change in $[Ca^{2+}]_i$ was followed by using Fura-2 ratio fluorescent microscopy. The $[Ca^{2+}]_i$ data plotted as a function of time are shown for nine βHC-13 CaBP40 cells. Data are representative of three experiments. Note the absence of an increase in $[Ca^{2+}]_i$ in response to high glucose in calbindin-D_{28k} overexpressing cells, but a very large increase in $[Ca^{2+}]_i$ with Ca^{2+} ionophore, ionomycin (5 μ*M*).

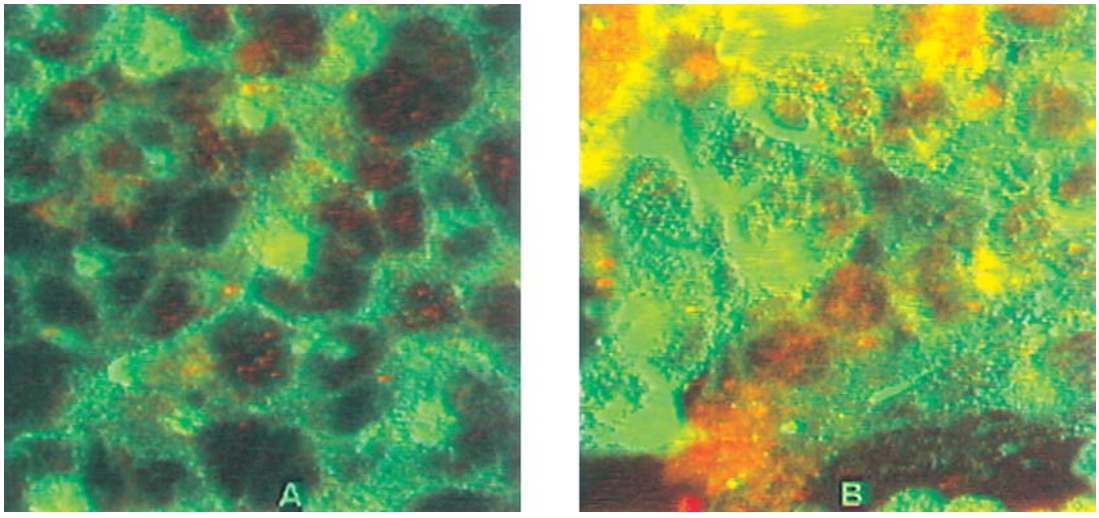

Fig. 5. Glucose-induced redistribution of calbindin-D_{28k} and its co-localization with L-type VDCC in βHC-13 CaBP40 cells. βHC-13 CaBP40 cells were either exposed to 30 m*M* glucose or remained in 5.5 m*M* glucose for 20 min and then the reaction was stopped in space and time by adding fixative. The fixed cells were labeled with antibodies directed against L-type VDCC and calbindin-D_{28k} and the secondary antibodies to these proteins contained Alexa Fluor 488 and Alexa Fluor 647 as fluorescent tags. The 3-D reconstruct of confocal images of cells in 5.5 m*M* glucose (panel A) indicates L-type VDCC (in green color) abundant in plasma membrane and calbindin-D_{28k} (in red color) primarily located in cytoplasm suggesting almost no co-localization of these proteins. In 30 m*M* glucose, the 3-D reconstruct (panel B) exhibits several areas of co-localization of these two proteins as shown by the appearance of yellow color (green + red = yellow). The height of the image stack is 10 μm. Each section in the stack was 1 μm.

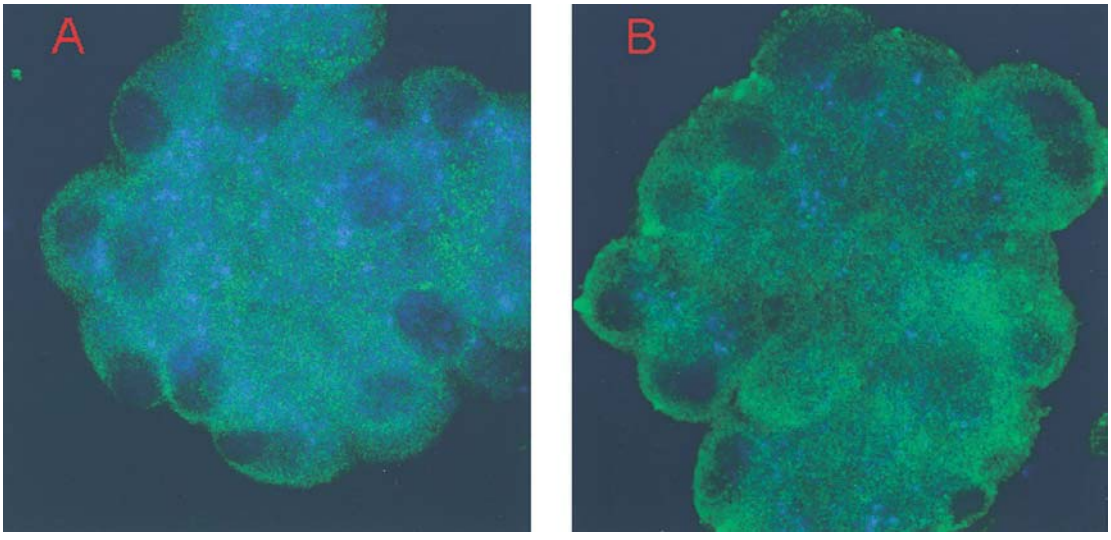

Fig. 6. Glucose-induced insulin release from calbindin-D_{28k} KO islets. KO islets incubated in 5.5 m*M* glucose were exposed to 30 m*M* glucose and the confocal images were acquired exactly as described in legend to the Fig. 5 except that the secondary antibody to insulin contained Alexa Fluor 568 as fluorescent probe. The 3-D reconstruct as shown in panel A in the presence of 5.5 m*M* glucose indicates an abundance of insulin secretory granules (shown in blue color) and L-type VDCC (shown in green color). In high glucose (panel B), the 3-D reconstruct clearly shows a decreased level of insulin granules in the KO islet (greatly reduced blue color).

in response to mobilization of Ca^{2+} from intracellular stores was also attenuated. A high concentration of ionomycin (5 μ*M*) overcame the buffering effect of calbindin-D_{28k} and produced a dramatic rise in $[Ca^{2+}]_i$. The finding of buffering of Ca^{2+} by moderately elevated levels of calbindin-D_{28k} in RIN cells was confirmed in RIN cells transfected with rat calbindin-D_{28k} and markedly overexpressing (>6- to 35-fold) this protein. These calbindin-D_{28k} transfected cells exhibited an increase in insulin mRNA and an increase in insulin content and insulin in the media *(18)*. Although Reddy et al. *(18)* found that the transfected RIN cells overexpressing calbindin-D_{28k} had increased insulin in the media, the physiological relevance of this finding was not known. It was noted that the calbindin-D_{28k}-overexpressing clones appeared to

preferentially release insulin, rather than store it, even though insulin content was found to be elevated. The authors stated that multiple factors including increased leakage and proteolysis could account for increased insulin in the media, suggesting release was not physiological. Nonetheless, the present study, both earlier studies *(17,18)*, and our more recent study *(5)* indicate the importance of calbindin-D_{28k} stabilizing intracellular levels of Ca^{2+}, specifically in the β-cell.

Evidence of calbindin-D_{28k} as a mediator of other rapid Ca^{2+} responses include translocation of Ca^{2+} in intestine *(42,43)*, activation of Ca^{2+}, Mg^{2+}-ATPase *(44)* and Ca^{2+}-ATPase and phosphodiesterase *(45)*, and altered Ca^{2+} fluxes in luminal vesicles of distal convoluted tubules *(46)*. Calcium as a second messenger encodes information in terms of magnitude (amplitude), frequency, and spatial organization of concentration changes *(47)*. Albritton et al. *(48)* showed that for cells the size of β-cells, Ca^{2+} as a messenger acted in very constrained domains. Hence, not only the amount, but also the intracellular location, of calcium-binding/regulatory proteins like calbindin-D_{28k} may be important in the transduction or translocation of localized bursts of intracellular free Ca^{2+} such as those resulting from release of Ca^{2+} from intracellular stores. It is conceivable that altered levels of calbindin-D_{28k} can lead to changes in glucose metabolism or glucose uptake that would affect insulin secretion. Zaitsev et al. *(49)* have suggested that the defective metabolism of glucose in islets from non-obese diabetic rats results in a delayed response to an increase in $[Ca^{2+}]_i$.

The mean basal $[Ca^{2+}]_i$ in βHC-13 and βHC-13 CaBP40 cells was about the same in spite of the fact that βHC-13 CaBP40 cells had an excess of calbindin-D_{28k} present. The maintenance of a basal $[Ca^{2+}]_i$ is very crucial for cell survival and cell division, and it would appear from our results that two explanations, which are not mutually exclusive, are likely. One, the high affinity binding sites on calbindin-D_{28k} are not completely active in basal conditions in binding the intracellular free Ca^{2+} and therefore they do not further buffer basal $[Ca^{2+}]_i$ and thus remain unsaturated with respect to Ca^{2+} binding. Two, the binding of free Ca^{2+} to high-affinity binding sites on calbindin-D_{28k} requires a driving force in terms of increased levels of $[Ca^{2+}]_i$ caused by glucose-induced membrane depolarization and influx of Ca^{2+} via L-type VDCC *(17,18)*. In earlier studies it was shown that calbindin-D_{28k} can protect β-cells from cytokine-mediated destruction by inhibiting free radical formation *(22)* and that overexpression of calbindin-D_{28k} in Sprague-Dawley rats led to neuroprotection against focal stroke *(50)*. Taken together the above studies indicate that calbindin-D_{28k} is involved in regulating as well as stabilizing the $[Ca^{2+}]_i$ in β-cells.

The basal insulin release rate as well as glucose-induced insulin release rate were significantly higher in βHC-13 control cells than in calbindin-D_{28k} overexpressing βHC-13 CaBP40 cells (Table 1). It is expected that calbindin-D_{28k} would bind some of the free Ca^{2+} obtained through the glucose-induced influx of Ca^{2+} via L-type VDCC and thereby decrease the rate of insulin release as observed in βHC-13 CaBP40 cells *(5,33–35)*. The existence of two distinct pools of insulin granules has been proposed by several research groups *(51–55)*. One pool, "primed" vesicles co-localized with Ca^{2+} channels, which are involved in the first phase of insulin release, and the other pool, "reserve" vesicles, which are not co-localized with Ca^{2+} channels, represents the second or prolonged phase of insulin release. Our data also suggest that there are probably two pools of insulin secretory granules, one (the primed vesicles) that is released at higher rates almost immediately upon addition of high glucose and contributes to the first phase of biphasic insulin secretion, and two, the reserve insulin pool that is released at comparatively lower rates (see Table 1) before the second phase of insulin secretion is sustained. These observations on insulin release from β-cell lines coincide very well with the glucose-induced temporal changes in $[Ca^{2+}]_i$ in islets derived from WT and KO mice (see Figs. 1A, B, and 2). However, in βHC-13 CaBP40 cells, the presence of excess calbindin-D_{28k} attenuates the glucose-induced rise in $[Ca^{2+}]_i$ perhaps due to the buffering action of this calcium-binding protein, and that in turn causes reduced rates of exocytosis of insulin granules (Table 1) thus further supporting a role of calbindin-D_{28k} in β-cell physiology.

The 3-D reconstructions of confocal images obtained from 5.5 m*M* glucose and 30 m*M* glucose-treated KO islets (Figs. 6A and B) indicated many more insulin granules in the former than in the later, thereby providing a visual display of the physiological action of glucose on insulin secretion. Confocal localization of molecules, such as insulin secretory granules, should prove useful in visualizing changes in signaling molecules and other modulators of β-cell function in addition to analyzing the effect of secretagogues on islet-cells.

From the novel results reported in Figs. 5A and B it is evident that some calbindin-D_{28k} upon binding free Ca^{2+}, which was derived from the glucose-induced influx of Ca^{2+} via L-type VDCC, moved from its primary location in the cytoplasm to the membrane regions that contained L-type VDCC (compare Figs. 5A and B). As mentioned above, βHC-13 CaBP40 cells were chosen because this cell line expressed high amounts of calbindin-D_{28k} and thus provided substantial immunofluorescent signal. The glucose-induced redistribution of calbindin-D_{28k} to co-localization with the L-type VDCC seems an important movement with regard to its regulatory functions, which may include influencing influx of Ca^{2+} via L-type VDCC and exocytosis of insulin granules. L-type VDCC are known to be localized to regions of the β-cell with a high concentration of insulin secretory granules *(56)*. It is possible that calbindin-D_{28k} associates with the excitosome (multiprotein complex) identified by Wiser et al. *(57)* as essential for exocytosis of insulin from

the β-cell. A number of studies have indicated that cytoplasmic free Ca^{2+} upon binding to one of the major calcium-binding proteins, calmodulin, causes conformational changes in calmodulin which then interacts with its specific target molecules *(58,59)*. Such a mechanism may also be hypothesized for calbindin-D_{28k} as is evident from the glucose-induced movement and co-localization of calbindin-D_{28k} and L-type VDCC presented in this study. Further experiments are certainly warranted to test the hypothesis and improve upon our understanding of the roles of calbindin-D_{28k} in pancreatic islet cells.

Materials and Methods

Animals

The experiments, utilizing wild type (WT) C57BL6 and knockout (KO) mice, were conducted in accord with the accepted standards of humane animal care as defined by the Institutional Animal Care and Use Committee of Joan C. Edwards School of Medicine at Marshall University, WV, USA.

Materials

Collagenase type V, ethyleneglycol-bis-(β-aminoethyl ether) *N*, *N*′-tetraacetic acid (EGTA), *N*-2-hydroxyethylpiperazine-*N*′-2-ethanesulfonic acid (HEPES), bovine serum albumin (BSA), ionomycin, dimethylsulfoxide (DMSO), the primary antibody against calbindin-D_{28k} (mouse anti-calbindin-D_{28k}), and $MnCl_2$ were obtained from Sigma Chemical Company (St. Louis, MO). Cell-Tak was purchased from Becton-Dickinson Labware (Bedford, MA). Dulbecco's Modified Eagle Medium (DMEM), heat-inactivated fetal bovine serum, heat inactivated horse serum, Hank's balanced salts solution (HBSS), penicillin-streptomycin, and geneticin were purchased from Gibco BRL (Gaithersburg, MD). Fura-2 acetoxy methylester (Fura-2AM), Pluronic F-127, fluorescent-labeled secondary antibodies Alexa Fluor 488 coupled to anti-rabbit IgG, Alexa Fluor 568 coupled to anti-guinea pig IgG, and Alexa Fluor 647 coupled to anti-mouse IgG were obtained from Molecular Probes Inc. (Eugene, OR). The primary antibody against L-type gated Ca^{2+} channel (Anti-α_{1C} L-type) was bought from Alomone Labs Ltd. (Jerusalem, Israel). The primary antibody against insulin (anti-porcine insulin) produced in guinea pig was purchased from Miles-Yeda Ltd (Rehovot, Israel). All other chemicals and reagents were of analytical grade.

Cell Culture

The βHC-13 cells were grown in 75 cm^2 tissue culture plates as well as on 25-mm-diameter coverslips placed in six-well tissue culture plates at 37ºC in a 5% CO_2–95% air incubator, with a modified DMEM medium supplemented with 17 m*M* glucose, 15% horse serum, 2.5% fetal bovine serum, 120 U/mL penicillin G, and 120 μg/mL streptomycin. The cell culture medium for the stably transfected βHC-13 CaBP40 cells also contained 800 μg/mL of geneticin.

Islet Preparation

The islets of Langerhans from the WT and KO mice were prepared by digesting the pancreatic tissue with collagenase followed by hand-picking the islets with a thin glass loop under a dissecting microscope as previously described *(60)*. The islets were incubated in a modified Kreb's ringer medium consisting of (in m*M*) 118 NaCl, 4.8 KCl, 1.5 $CaCl_2$, 1.2 $MgCl_2$, 1.2 KH_2PO_4, 10 HEPES, 5 $NaHCO_3$, 5.5 glucose, and 0.1% w/v BSA, pH 7.40.

$[Ca^{2+}]_i$ Measurements

The $[Ca^{2+}]_i$ in islets, βHC-13 cells, and βHC-13 CaBP40 cells was determined by using ratio fluorescence microscopy procedure of Fura-2 loaded islets or β-cells and is described below in brief:

Dye-loading: The islets were incubated with 5 μ*M* Fura-2AM and 0.05% (w/v) Pluronic F-127 for 45–50 min at 37ºC followed by thrice washing with HBSS and incubating further for 10–15 min at 37ºC. The islets were then suspended in a small volume (50–100 μL) of HBSS and placed onto the Cell-Tak coated coverslips to allow them to adhere to the surface for 10–15 min at room temperature and finally 1 mL of the complete modified Kreb's ringer medium containing 2.8 m*M* glucose was added. The βHC-13 control cells and βHC-13 CaBP40 cells were loaded with 5 μ*M* Fura-2AM and 0.05% (w/v) Pluronic F-127 for 30 to 35 min at 37ºC followed by washing with HBSS and further incubation in HBSS at 37ºC for 10 to 15 min. The cells were finally incubated in HBSS.

Digital Video Fluorescence Imaging: The Narishige microincubation chamber containing Fura-2 loaded islets or β-cells was placed on the stage of a Nikon Diaphot TMD inverted fluorescence microscope (Nikon Corporation, Tokyo, Japan) equipped for ratio fluorescence microscopy, which was carried out at 37ºC. The samples were then successively excited at 340 and 380 nm and the fluorescence emitted at 510 nm was intensified by a DAGE-MTI GenIISys image intensifier and finally captured by a DAGE-MTI CCD72 video camera (DAGE-MTI, Inc., Michigan City, IN). Metafluor Imaging System software version 4.1.7 (Universal Imaging Corporation, Westchester, PA) was used for image acquisition and analysis. The $[Ca^{2+}]_i$ was calculated according to the equation used by Grynkiewicz et al. *(61)*. All images were corrected for the background emission.

Triple Fluorescent Antibodies Labeling and Laser Scanning Confocal Microscopy

The βHC-13 CaBP40 cells grown onto 25-mm-diameter coverslips and islets stabilized on Cell-Tak coated coverslips were each incubated in 2 mL of HBSS in a six-well culture plate. To two of the coverslips, one containing βHC-13 CaBP40 cells and the other containing islets, small aliquots

of stock glucose solution were added to a final concentration of 30 m*M*, whereas the other two coverslips, one containing βHC-13 CaBP40 cells and the other containing islets, were incubated with 5.5 m*M* glucose that served as appropriate controls. The incubation with high glucose and corresponding control was carried out at 37ºC for a period of 20–25 min. The reaction was stopped in space and time by adding 4% (w/v) freshly prepared paraformaldehyde as a fixative.

The fixed islets and βHC-13 CaBP40 cells were then treated with primary antibodies against calbindin-D_{28k}, L-type gated Ca^{2+} channels, and insulin. The treatment with the fluorescent-labeled secondary antibodies against primary antibodies was done by incubating the coverslips with Alexa Fluor 488 coupled to anti-rabbit IgG, Alexa Fluor 568 coupled to anti-guinea pig IgG, and Alexa Fluor 647 coupled to anti-mouse IgG. The confocal fluorescence images of the triple fluorescent labeled proteins were scanned by using a Bio-Rad MRC 1024 Laser Scanning Confocal Microscope (Bio-Rad, Microscopy Division, Hemel Hempstead Herts, England). Confocal image acquisition and analysis was carried out using an in-built Laser Sharp 3.2 software from Bio-Rad as well as Confocal Assistant version 4.02 (Todd Clark Brelje) and Metamorph version 4.1.7 software (Universal Imaging Corp., Westchester, PA).

Insulin Release Assay

The glucose-induced insulin release from the βHC-13 control cells and βHC-13 CaBP40 cells was determined at 37ºC by using a competitive enzyme-linked immunosorbent assay (ELISA) protocol modified in our laboratory from that of Kekow et al. *(62)*.

Statistical Analysis

The statistical significance of the results was analyzed by using Student's *t* test (SigmaStat software, Jandel Scientific Software, San Rafael, CA).

Acnowledgments

This work was supported by NIH grants DK54033, DK38961, and DK98007.

References

1. Sergeev, I. N. and Rhoten, W. B. (1995). *Endocrinology* **136,** 2852–2861.
2. Putney, J. (1999). *Proc. Natl. Acad. Sci. USA* **96,** 14,669–14,671.
3. Brown, E. M. and MacLeod, R. J. (2000). *Physiol. Rev.* **81,** 239–287.
4. Li, C., Fultz, M. E., Parkash, J., Rhoten, W. B., and Wright, G. L. (2001). *J. Muscle Res. Cell Motil.* **22,** 521–534.
5. Sooy, K., Schermerhorn, T., Noda, M., et al. (1999). *J. Biol. Chem.* **274,** 34,343–34,349.
6. Airaksinen, M. S., Eilers, J., Garaschuk, O., Thoenen, H., Konnerth, A., and Meyer, M. (1997). *Proc. Natl. Acad. Sci. USA* **94,** 1488–1493.
7. Sergeev, I. N. and Rhoten, W. B. (1998). *Endocrine* **9,** 321–327.
8. Rhoten, W. B., Bruns, M. E. H., and Christakos, S. (1985). *Endocrinology* **117,** 674–683.
9. Christakos, S., Gabrielides, C., and Rhoten, W. B. (1989). *Endocr. Rev.* **10,** 3–26.
10. Heizmann, C. W. and Hunziker, W. (1991). *Trends Biochem. Sci.* **16,** 98–103.
11. Zimmer, D. B., Chessher, J., Wilson, G. L., and Zimmer, W. E. (1997). *Endocrinology* **138,** 5176–5183.
12. Wagner, L., Oliyarnyk, O., Gartner, W., et al. (2000). *J. Biol. Chem.* **275,** 24,740–24,751.
13. Varghese, S., Deaven, L. L., Huang, Y. C., et al. (1989). *Mol. Endocrinol.* **3,** 495–502.
14. Minghetti, P. P., Cancela, L., Fujisawa, Y., Theofan, G., and Norman, A. W. (1988). *Mol. Endocrinol.* **2,** 355–367.
15. Wilson, P. W., Rogers, J., Harding, M., Pohl, V., Pattyn, G., and Lawson, D. E. (1988). *J. Mol. Biol.* **200,** 615–625.
16. Hunziker, W. (1986). *Proc. Natl. Acad. Sci. USA* **83,** 7578–7582.
17. Rhoten, W. B. and Sergeev, I. N. (1994). *Endocrine* **2,** 989–995.
18. Reddy, D., Pollock, A. S., Clark, S. A., et al. (1997). *Proc. Natl. Acad. Sci. USA* **94,** 1961–1966.
19. Rintoul, G. L., Raymond, L. A. and Baimbridge, K. G. (2001). *Cell Calcium* **29,** 277–287.
20. Bellido, T., Huening, M., Raval-Pandya, M., Manolagas, S. C., and Christakos, S. (2000). *J. Biol. Chem.* **275,** 26,328–26,332.
21. Airaksinen, L., Virkkala, J., Aarnisalo, A., Meyer, M., Ylikoski, J., and Airaksinen, M. S. (2001). *ORL J. Otorhinolarygol. Relat. Spec.* **62,** 9–12.
22. Rabinovitch, A., Suarez-Pinzon, W. L., Sooy, K., and Christakos, S. (2001). *Endocrinology* **142,** 3649–3655.
23. Radvanyi, F., Christgau, S., Baekkeskov, S., Jolicoeur, C., and Hanahan, D. (1993). *Mol. Cell. Biol.* **13,** 4223–4232.
24. Schuit, F. C., Huypens, P., Heimberg, H., and Pipleers, D. G. (2001). *Diabetes* **50,** 1–11.
25. Schofl, C., Borger, J., Lange, S., Muhlen, A. V. Z., and Brabant, G. (2000). *Endocrinology* **141,** 4065–4071.
26. Prentki, M. and Matschinky, F. M. (1987). *Physiol. Rev.* **67,** 1185–1248.
27. Aguilar-Bryan, L., Clement, J. P., Gonzalez, G., Kunjilwar, K., Babenko, A., and Bryan, J. (1998). *Physiol. Rev.* **78,** 227–245.
28. Seino, S. (1999). *Annu. Rev. Physiol.* **61,** 337–362.
29. Theler, J.-M., Mollard, P., Guerineau, N., et al. (1992). *J. Biol. Chem.* **267,** 18,110–18,117.
30. Antunes, C. M., Salgado, A. P., Rosario, L. M., and Santos, R. M. (2000). *Diabetes* **49,** 2028–2038.
31. Leech, C. A., Holz, G. G. IV, and Habener, J. F. (1994). *Endocrinology* **135,** 365–372.
32. Dukes, I. D., Roe, M. W., Worley, J. F., and Philipson, L. H. (1997). *Curr. Opin. Endocr. Diabetes* **4,** 262–271.
33. Jones, P. M. and Persaud, S. J. (1998). *Endocr. Rev.* **19,** 4229–4261.
34. Easom, R. A. (1999). *Diabetes* **48,** 675–684.
35. Lang, J. (1999). *Eur. J. Biochem.* **259,** 3–17.
36. Duchen, M. R., Smith, P. A., and Ashcroft, F. M. (1993). *Biochem. J.* **294,** 35–42.
37. Martin, F., Reig, J. A., and Soria, B. (1995). *J. Mol. Endocrinology* **15,** 177–185.
38. Bertuzzi, F., Davalli, A. M., Nano, R., et al. (1999). *Diabetes* **48,** 1971–1978.
39. Van Eylen, F., Lebeau, C., Albuquerque-Silva, J., and Herchuelz, A. (1998). *Diabetes* **47,** 1873–1880.
40. Gopel, S. O., Kanno, T., Barg, S., et al. (1999). *J. Gen Physiol.* **114,** 759–770.
41. Leach, C. A. and Habener, J. F. (1998). *Diabetes* **47,** 1066–1073.
42. Nemere, I., Leathers, V., and Norman, A. W. (1986). *J. Biol. Chem.* **261,** 16,106–16,114.
43. Nemere, I., Leathers, V. L., Thompson, B. S., Luben, R. A., and Norman, A. W. (1991). *Endocrinology* **129,** 2972–2984.

44. Morgan, D. W., Welton, A. F., Heick, A. E., and Christakos, S. (1986). *Biochem. Biophys. Res. Commun.* **138,** 547–553.
45. Reisner, P. D., Christakos, S., and Vanaman, T. C. (1992). *FEBS Lett.* **297,** 127–131.
46. Bouhtiauy, I., Lajeunesse, D., Christakos, S., and Brunette, M. G. (1994). *Kidney Int.* **45,** 461–468.
47. Leichleiter, J., Girard, S., Peralta, E., and Clapham, D. (1991). *Science* **252,** 123–126.
48. Albritton, N. L., Meyer, T., and Stryer, L. (1992). *Science* **258,** 1812–1815.
49. Zaitsev, S., Efanova, I., Ostenson, C. G., Efendic, S., and Berggren, P. O. (1997). *Biochem. Biophys. Res. Commun.* **239,** 129–133.
50. Yenari, M. A., Minami, M., Sun, G. H., et al. (2001). *Stroke* **32,** 1028–1035.
51. Rorsman, P., Eliasson, L., Renstrom, E., Gromada, J., Barg, S., and Gopel, S. (2000). *News Physiol. Sci.* **15,** 72–77.
52. Barg, S., Eliasson, L., Renstrom, E., and Rorsman, P. (2002). *Diabetes* **51,** S74–S82.
53. Nesher, R., Anteby, E., Yedovizky, M., Warwar, N., Kaiser, N., and Cerasi, E. (2002). *Diabetes* **51,** S68–S73.
54. Henquin, J.-C., Ishiyama, N., Nenquin, M., Ravier, M. A., and Jonas, J.-C. (2002). *Diabetes* **51,** S60–S67.
55. Nesher, R. and Cerasi, E. (2002). *Diabetes* **51,** S53–S59.
56. Bokvist, I., Eliasson, L., Ammala, C., Renstrom, E., and Rorsman, P. (1995). *EMBO J.* **14,** 50–57.
57. Wiser, O., Trus, M., Hernandez, A., et al. (1999). *Proc. Natl. Acad. Sci. USA* **96,** 248–253.
58. Crivici, A. and Ikura, M. (1995). *Annu. Rev. Biophys. Biomol. Struct.* **24,** 85–116.
59. Weinstein, H. and Mehler, E. L. (1994). *Annu. Rev. Physiol.* **56,** 213–236.
60. Clements, R. S. and Rhoten, W. B. (1976). *J. Clin. Invest.* **57,** 684–691.
61. Grynkiewicz, G., Poenie, M., and Tsien, R. Y. (1985). *J. Biol. Chem.* **260,** 3440–3450.
62. Kekow, J., Ulrichs, K., Muller-Ruchholtz, W., and Gross, W. L. (1988). *Diabetes* **37,** 321–326.